ACCSCIENCE PUBLISHING

International Journal of Bioprinting

RESEARCH ARTICLE

Manipulating fungal growth in engineered living materials through precise deposition of nutrients

Supplementary File

(A) Effect of carboxymethyl cellulose on the extrudability of the ink

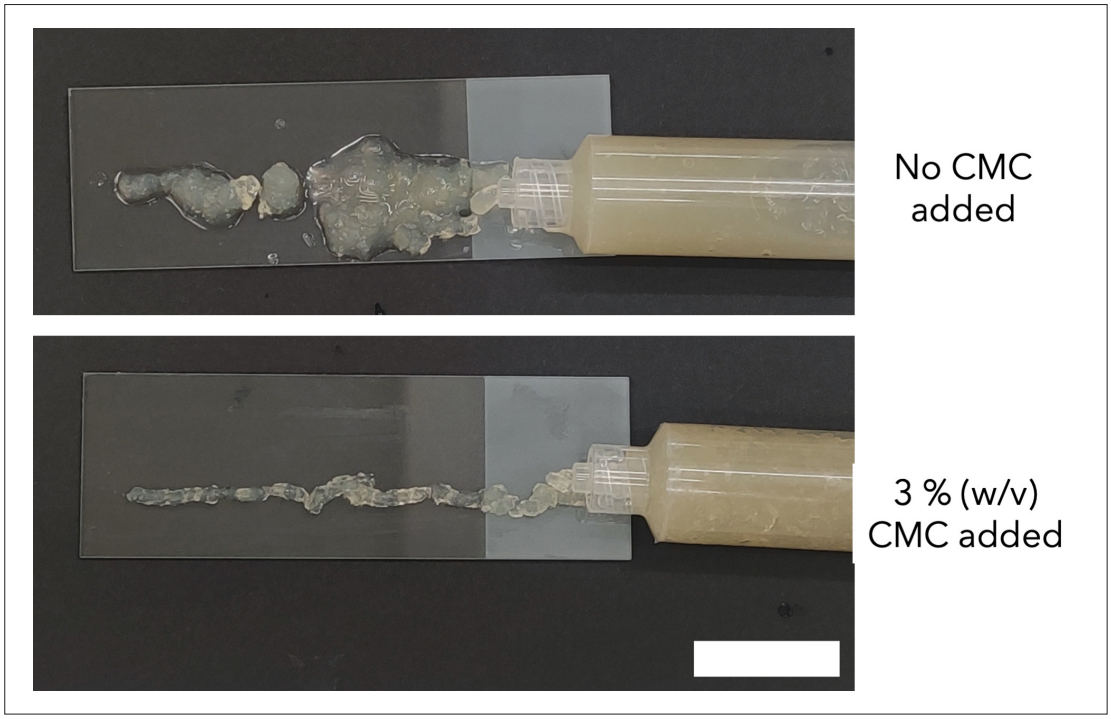

Figure S1. Effect of carboxymethyl cellulose (CMC) on the extrudability of the ink. Filaments formed from extruding an ink devoid of CMC (2.5% w/v agar + 1% w/v alginate, top panel) and another ink with the same composition as above but containing an additional 3% w/v CMC (bottom panel) through the 1.5 mm (ID) open end of a syringe, respectively. Scale bars: 20 mm.

(B) Two-level full factorial design to study the effects of each component on the rheology of the overall ink

To study the effects of each component on the rheology of the overall ink, a two-level full factorial design of experiment was conducted (Figure S2). Since the ink consists of three components, $2^3 = 8$ different formulations were made in this design of experiment.

Inks were prepared by dissolving alginate and carboxymethyl cellulose (CMC) first in a solution of malt (2% w/v) and peptone (0.1% w/v) under magnetic stirring at 45°C. Agar was then added and the temperature of the mixture was raised to facilitate the dissolution of agar. The mixture was then autoclaved at 121°C for 20 min, and once removed from the autoclave, it was stirred until it had set. Inks were prepared with concentrations of agar, alginate, and CMC according to the schematics shown in Figure S2 (left panel).

The rheological properties of the inks were evaluated using a Bohlin Gemini HR Nano rheometer (Malvern, UK). A 15 mm serrated plate and a measuring gap of 0.5 mm were used. Samples were pre-sheared using a shear rate of 10 s^{-1} for 30 s before being allowed to equilibrate for 60 s. For steady-state viscosity tests, a shear rate range of 0.01–1000 s^{-1} was used. The viscosity as a function of shear rate was then recorded and was fitted to the non-Newtonian power law model, which is given by **Equation S1**:

$$\mu = K\dot{\gamma}^{n-1} \quad \text{(S1)}$$

where μ is the apparent viscosity, K is the flow consistency index, $\dot{\gamma}$ is the shear rate, and n is the flow behavior index.

For amplitude sweep tests, using a frequency of 0.5 Hz, the shear stress was increased from 0.1 Pa up until the flow point of the ink was reached. If the ink has no flow point, the shear stress was increased until the yield point was exceeded instead. The storage and loss moduli were then recorded. For samples with very low viscosity, a frequency of 0.1 Hz was used instead. From the storage and loss moduli, the yield point and the flow point were identified. The yield point is defined as the shear rate corresponding to the upper limit of the linear viscoelastic region (the point at which the decrease in storage modulus is 5%). The flow point is defined as the shear stress corresponding to the point of intersection between the storage modulus and the loss modulus.[1] A flow point of 0 was designated to samples that have loss modulus higher than their respective storage moduli regardless of the shear stress.

All samples were tested at 25°C. Triplicates of each sample were analyzed. Statistical analyses were conducted using a three-way analysis of variance (ANOVA) with a significance level of 0.05.

Based on Figure S3, agar had the most significant contribution to the rheology of the ink as an increase in agar resulted in a large increase in the flow consistency index (which corresponds to higher viscosity), yield point (which corresponds to the rigidity of the printed structure), and flow point (which corresponds to the pressure required to extrude the ink). Agar also reduced the flow behavior index, indicating that the ink is more shear-thinning as more agar is added. This is followed by CMC. While its contribution to the flow point was statistically insignificant (p >0.05), increasing the concentration of CMC resulted in a significant increase in the flow consistency index and the yield point of the overall ink. However, its addition reduced the shear-thinning properties of the ink by increasing the flow behavior index. Meanwhile, alginate provided the least contribution to the flow consistency index, and increasing its concentration even decreased the yield point and the flow point of the ink. While alginate may help improve the viscosity of the overall ink, its inclusion was shown to be detrimental to the rigidity of the ink and subsequently, the overall structure.

Besides the main effects, the interaction effects between different components of the inks should be investigated as the presence of certain components may result in others having different magnitudes in their respective main effects (Figure S4). The contribution by agar toward the flow point of the overall ink was independent of the concentration level of CMC. This means CMC neither

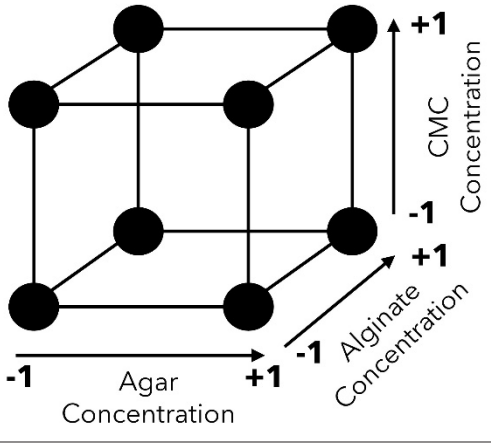

Level	Concentration [% (w/v)]
Low (-1)	0.1
High (+1)	3

Figure S2. A two-level full-factorial design was used to investigate the contribution of each component toward the rheology of the overall ink. (Left) Schematic of the two-level full factorial design of experiment used to study the contribution of each ink components toward the rheology of the overall ink. As a result, eight different samples sets were tested. (Right) The concentration at both low and high levels of each component.

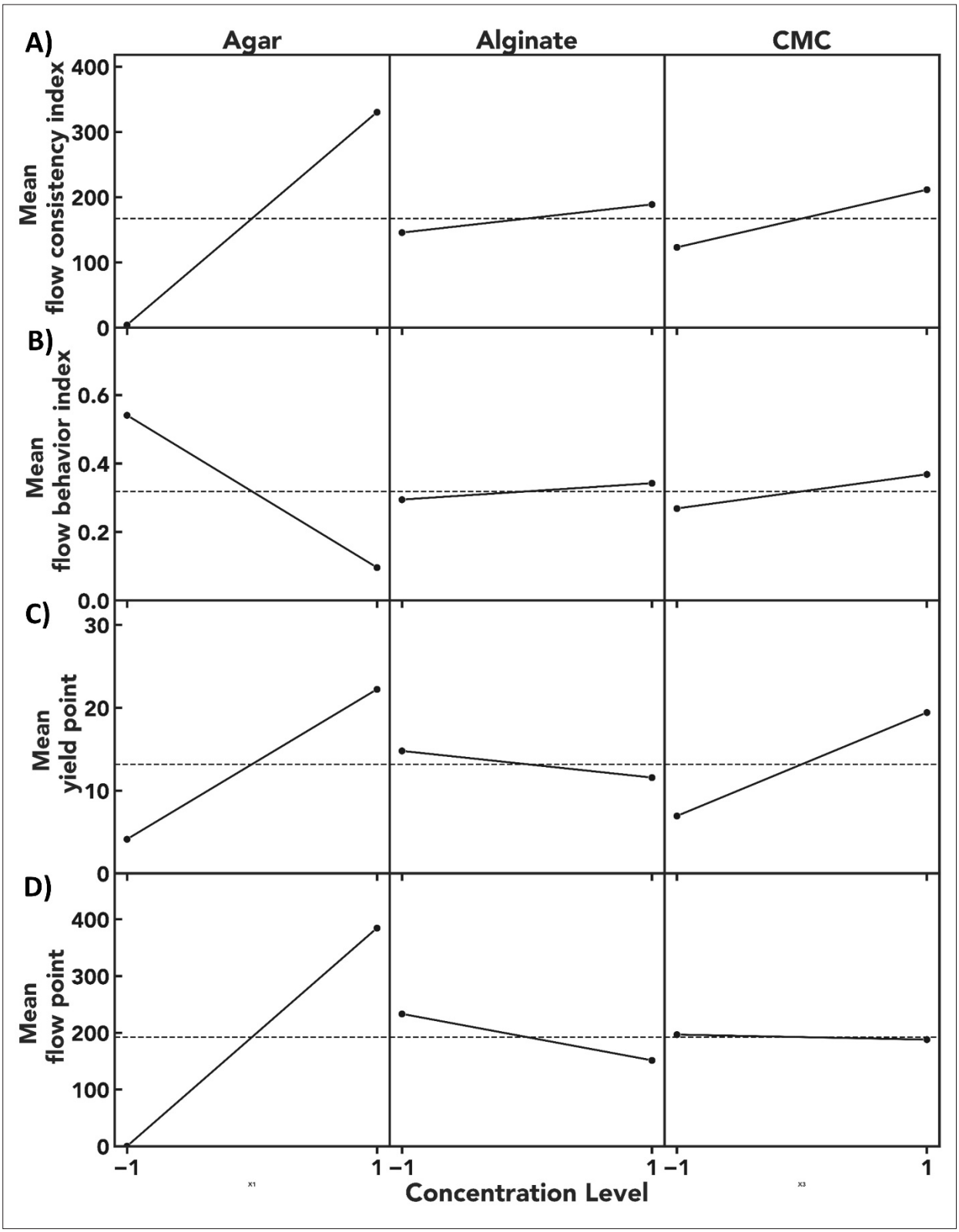

Figure S3. Each component has significant effects on the rheology of the overall ink. Main effects plot indicating the effects of agar, alginate, and carboxymethyl cellulose (CMC) respectively on the flow consistency index (A), flow behavior index (B), yield point (C), and flow point of the overall ink (D). The dotted horizontal line represents the corresponding average values of all the eight sample groups tested.

improved nor reduced the contribution of agar toward increasing the flow point. The magnitude of increase in the flow consistency index caused by agar was greater at high concentration levels of alginate and CMC, respectively. Meanwhile, alginate reduced the magnitude of change in the other rheological properties caused by agar, indicating a form of anti-synergy between agar and alginate. While the addition of alginate was likely to reduce the viscosity, yield point, and flow point of the ink, the addition of CMC reversed this trend when it comes to the flow consistency index, flow behavior index, and flow point. However, the effect that alginate has in decreasing the yield point of the overall ink was independent of the concentration of CMC inside the ink.

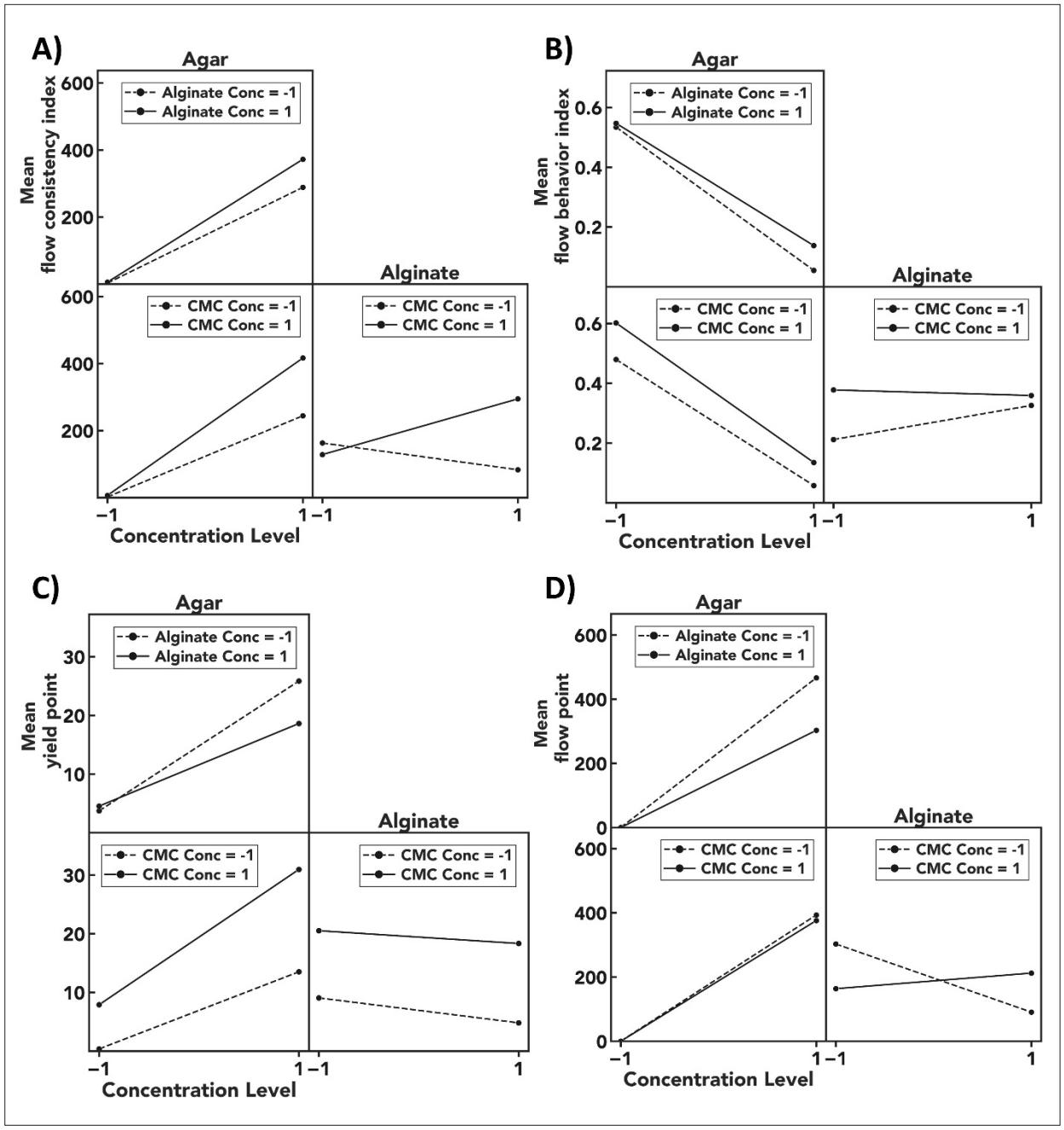

Figure S4. Interactions between different components have an effect on the rheology of the overall ink. Interaction effects plots indicating the effects of different components at different concentration levels on the flow consistency index (A), flow behavior index (B), yield point (C), and flow point of the overall ink (D).

(C) Shape fidelity of mycelium ink

(D) Effect of macropore size on mycelium growth on mycelium-based engineered living materials

(E) Growth of mycelium on agar containing various levels of malt and peptone

(F) Hydrophobicity of mycelium sheets grown on agar containing different levels of malt and peptone

Hydrophobicity of mycelium sheets grown on agar containing varying levels of malt and peptone, respectively, was evaluated using a contact angle goniometer (OCA15 DataPhysics Instruments, Germany). Pure mycelium sheets were affixed onto glass slides using double-sided tape. Deionized water (6 μL) was then dispensed on the mycelium sheet and the contact angle on both sides of the droplet was measured. The average contact angle between both sides was then calculated and reported. Five replicates

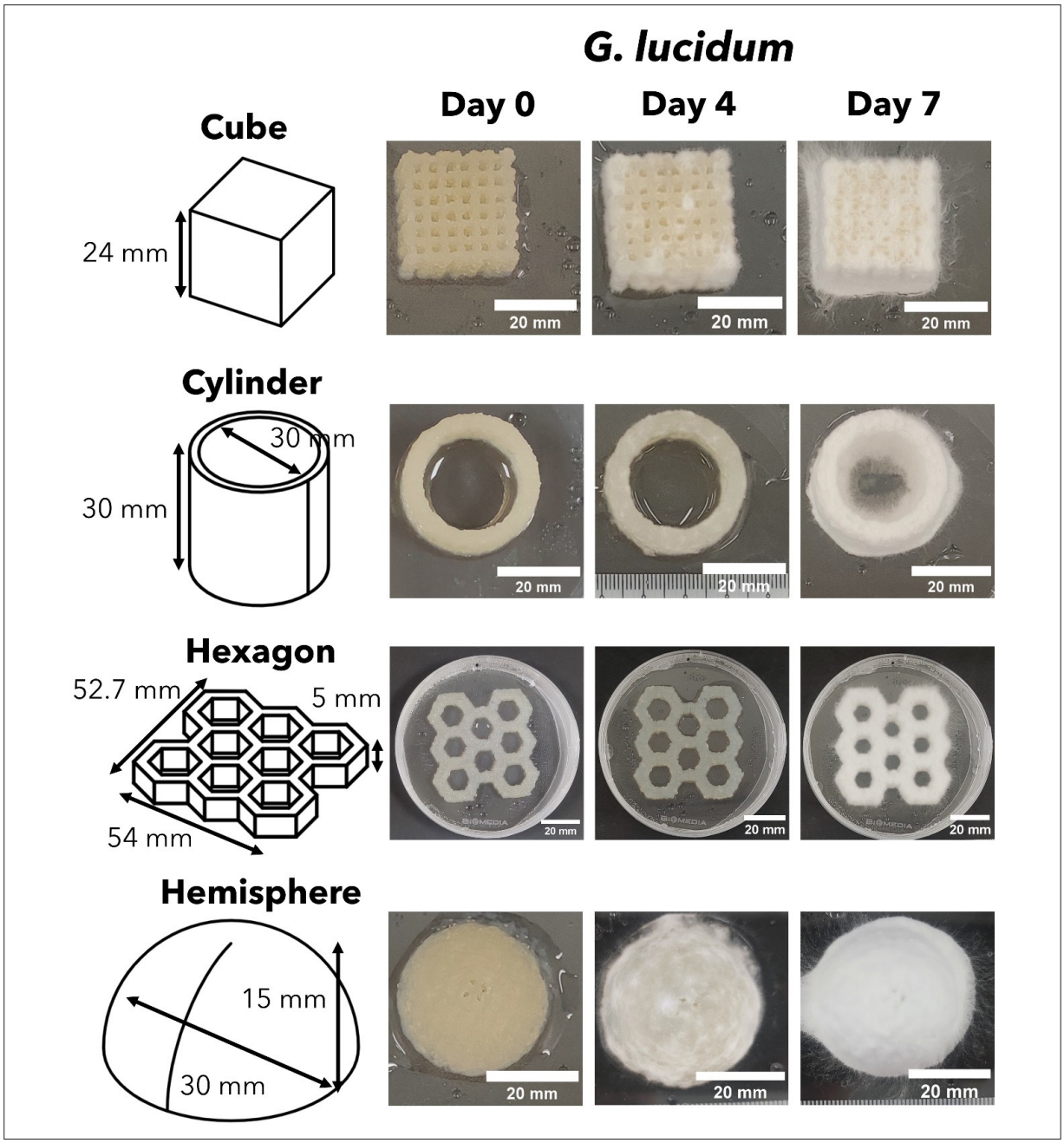

Figure S5. Mycelium-based engineered living materials (ELMs) can be printed in various shapes with high shape fidelity. Digital images of the growth of *G. lucidum* in 3D-printed constructs of various shapes over a period of 7 days.

were obtained from each sample. Statistical analysis was conducted using a two-way ANOVA with a significance level of 0.05, followed by a post hoc Tukey's HSD test. Values are expressed as mean ± standard deviation.

Based on Figure S8, for *P. ostreatus*, an increase in both malt and peptone concentration in the substrate resulted in an increase in contact angle at low levels of malt and peptone concentration. This observation seems to support the hypotheses that a greater network density caused by increased malt availability contributes to the film being more hydrophobic, and also that more hydrophobins (proteins responsible for the hydrophobic behavior of mycelium) are synthesized by the mycelium

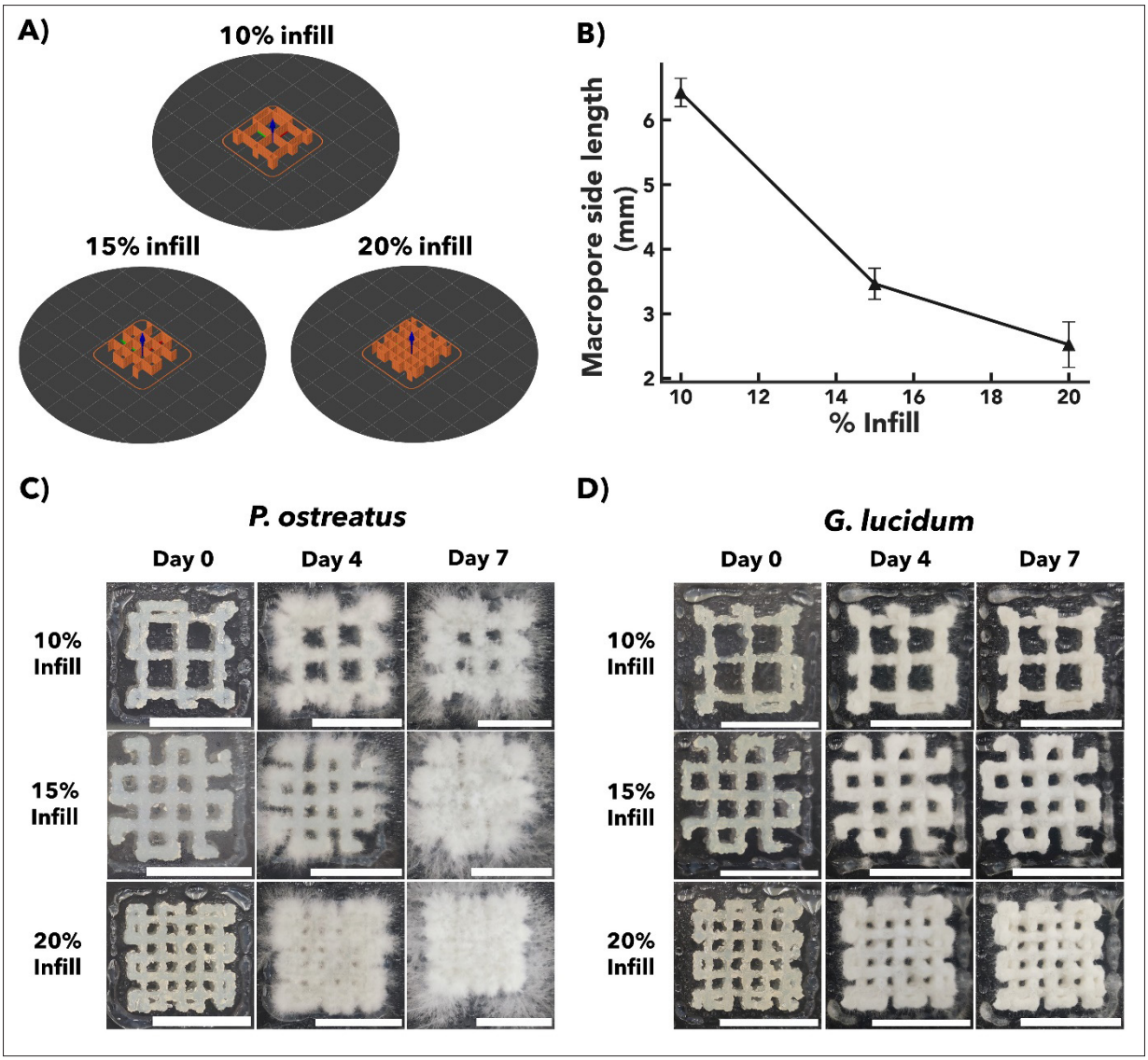

Figure S6. Effect of macropores size on mycelium growth on mycelium-based engineered living materials (ELMs). (A) Various percentage infills on the same geometry (20 × 20 × 5 mm^3 cuboid). A grid pattern is used as the infill. (B) Size of macropores of each percentage infill. Digital images of the growth of (C) *P. ostreatus* and (D) *G. lucidum* in 3D-printed constructs of various infills, respectively, over a period of 7 days. Scale bars: 20 mm.

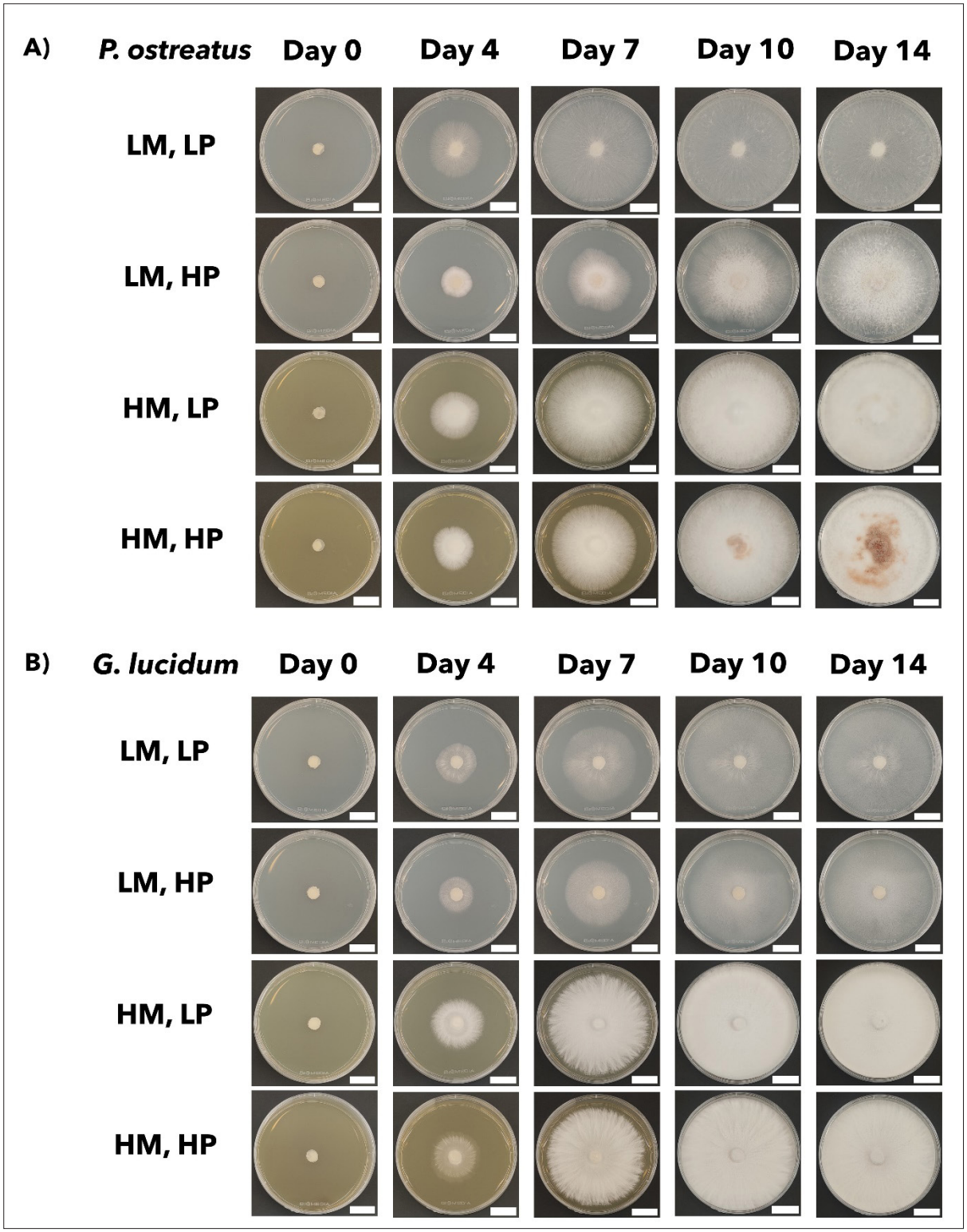

Figure S7. Time-lapse examination of mycelium growth on agar containing varying levels of malt and peptone, respectively. Digital images of *P. ostreatus* (A) and *G. lucidum* (B) grown on agar plates containing varying levels of malt and peptone, respectively, over a period of 14 days. Abbreviations: HM, high malt (5% w/v); HP, high peptone (1% w/v); LM, low malt (0.1% w/v); LP, low peptone (0.01% w/v). Scale bars: 20 mm.

when a more abundant protein source is available. However, quantification of hydrophobins produced is required to validate this inference. As for *G. lucidum*, it can be hypothesized that the variation in concentration of nutrients is not sufficient to elicit a significant change in the synthesis of hydrophobins across all sample groups, resulting in consistent hydrophobicity across all groups.

(G) Additional multi-material fungal-based engineered living materials

(H) Supplementary videos

Video S1. Time-lapse video of mycelium growth of *P. ostreatus* on agar containing varying levels of malt and peptone.

Video S2. Time-lapse video of mycelium growth of *G. lucidum* on agar containing varying levels of malt and peptone.

References

1. Amplitude sweeps | Anton Paar Wiki. Anton Paar. Accessed April 3, 2024. https://wiki.anton-paar.com/ca-en/amplitude-sweeps/

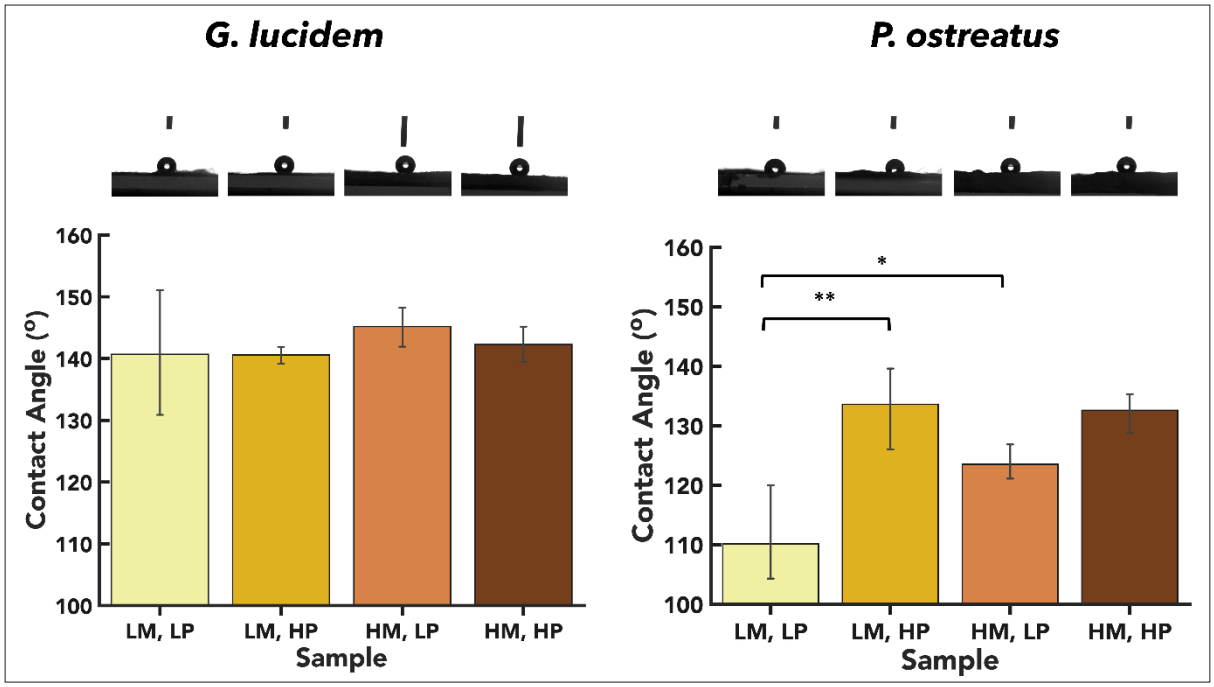

Figure S8. Hydrophobicity of mycelium sheets grown on agar containing different levels of malt and peptone, respectively. Contact angle on *G. lucidum* and *P. ostreatus* mycelia grown on agar containing varying concentrations of malt and peptone, respectively. Abbreviations: HM, high malt (5% w/v); HP, high peptone (1% w/v); LM, low malt (0.1% w/v); LP, low peptone (0.01% w/v). *$p < 0.05$, **$p < 0.01$.

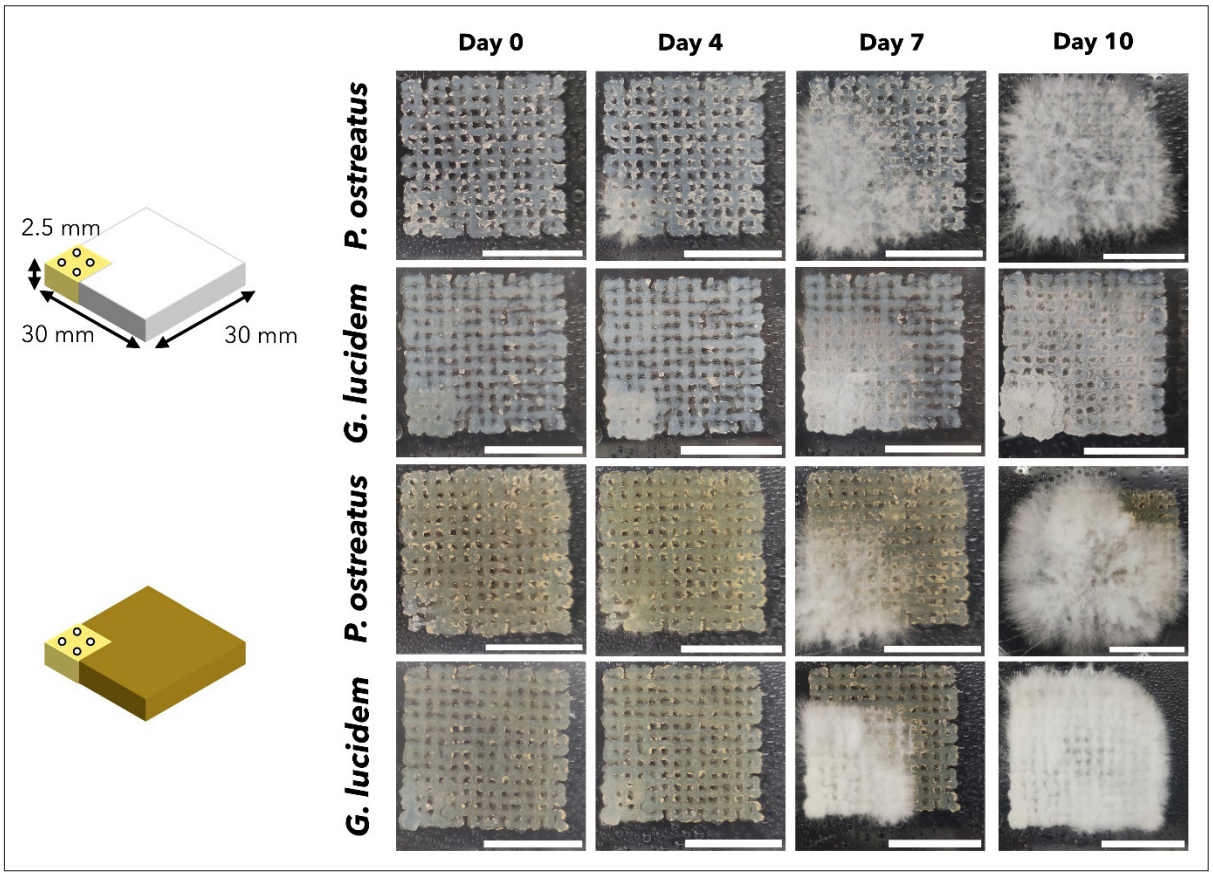

Figure S9. Foraging behavior of mycelium of *P. ostreatus* and *G. lucidum* on two-dimensional surface containing either low malt content (the top two rows) or high malt content (the bottom two rows), respectively. Scale bars: 20 mm.

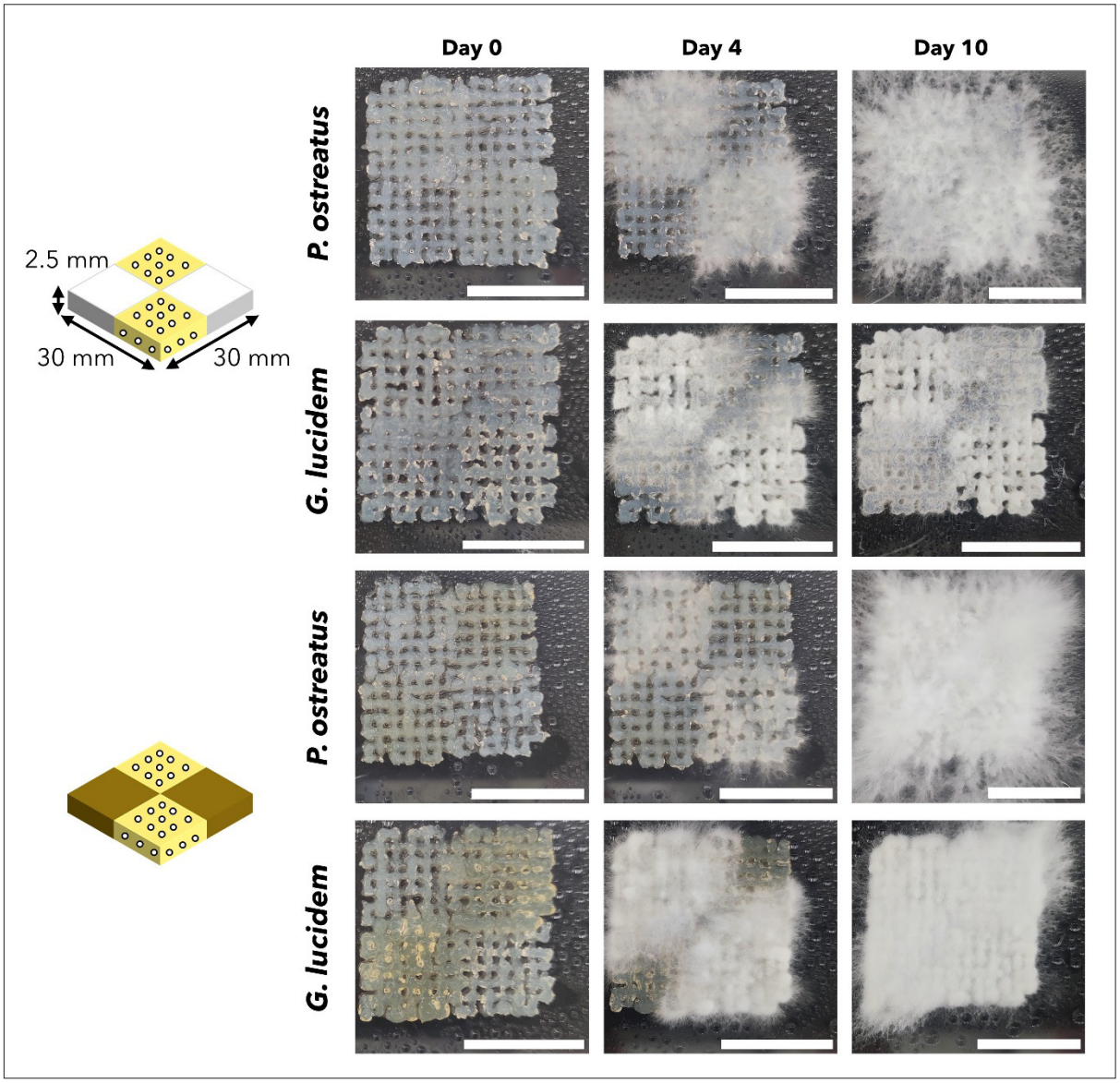

Figure S10. Foraging behavior of mycelium of *P. ostreatus* and *G. lucidum* on complex patterned surfaces containing zones of either low malt content (the top two rows) or high malt content (the bottom two rows) respectively. Scale bars: 20 mm.